The Effect of Atmospheric Haze on Infrared Radiative Cooling Rates

WILFORD ZDUNKOWSKI, DONALD HENDERSON AND J. VERN HALES[1]

Intermountain Weather, Inc.,[2] and University of Utah, Salt Lake City

(Manuscript received 2 April 1965, in revised form 6 December 1965)

ABSTRACT

The radiative flux divergence is computed for the lower few centimeters of the atmosphere assuming a water vapor-haze mixture. Some additional computations are made for higher altitudes also. The haze model, based on Deirmendjian's formulation, is used to obtain the scattering and absorption coefficients from Mie theory, which are employed in radiative transfer equations. This new formulation of the radiative transfer equation takes into consideration the combined effects of water vapor and particle absorption, as well as primary particle scattering. The influence of the albedo of the earth and the interface temperature discontinuity is taken into consideration. Results show that the incorporation of a reasonable interface temperature discontinuity of the earth's surface is of higher order of importance than the haze influence near the surface.

1. Introduction

The temperature changes near the surface due to water vapor alone have been investigated, for example, by Fleagle (1953), Möller (1955), Hales *et al.*[3] and Zdunkowski and Johnson (1965). Although various degrees of sophistication were used in the later models, no attempt was made by any of these authors to include the effect of atmospheric haze. The possible effects of this haze upon the heat regime have been pointed out only qualitatively. Now the attempt shall be made to include the effect of haze assuming a continuous haze distribution which decreases exponentially with height as well as layered haze.

Water vapor and temperature distribution curves are available from standard measurements, and water vapor emission data sufficiently accurate for this purpose are also available. Haze distribution curves, however, are difficult to obtain and one has to refer to models. Such a model representing continental conditions has been described by Deirmendjian (1959) and will be used in this investigation. It should be noted that the haze model is based on actual particle counts.

2. Haze extinction coefficients

In order to make calculations, the extinction coefficients for haze particles must be available. Since an exact description of the physical properties of these particles is not known, it is assumed, as Deirmendjian did, that all particles are water droplets so that the known values of the complex index of refraction for water may be used to compute the extinction and absorption efficiency factors by means of Mie theory. This conclusion agrees with the results of Volz (1957), whose measurements unfortunately only cover the region up to approximately 15 microns.

Calling L the monochromatic extinction coefficient for haze and μ the mass of the haze, then the optical path length of haze can be written as

$$L\mu=\left|\int_{z_1}^{z}\beta_{\text{ext}}dz\right|, \tag{1}$$

where z_1 stands for the height of the reference level and z is the variable height coordinate. β_{ext} is the monochromatic haze extinction coefficient per unit length and is defined in such a manner that it may be derived from $\beta_{0,\text{ext}}$, the extinction coefficient at the surface of the earth, by means of

$$\beta_{\text{ext}}=\beta_{0,\text{ext}}e^{-z/H}. \tag{2}$$

Here H stands for the height of the homogeneous haze atmosphere. The monochromatic extinction coefficient β_0 is computed from

$$\beta_{0,\text{ext}}=\pi\int_{r_1}^{r_2}n(r)r^2Q_{\text{ext}}(\alpha,\lambda)dr. \tag{3}$$

Here α is the size parameter $2\pi r/\lambda$ with r the particle radius and λ the wavelength of the incoming radiation. The particle distribution n is defined by

$$n(r)=2.251r^{-4} \qquad [\text{cm}^{-3}\,\mu^{-1}] \quad \text{for} \quad r_0\leqq r\leqq r_2,$$

[1] Present affiliation: General Electric Company, Valley Forge Space Technology Center, Philadelphia, Pa.

[2] The research reported in this document has been sponsored by the U. S. Army Electronics Command, Fort Monmouth, N. J., under Contract No. DA 28-043 AMC-00122(E).

[3] Hales, J. V., W. Zdunkowski and D. Henderson, 1965: Flux divergence in a multiple component non-scattering atmosphere. (To be published.)

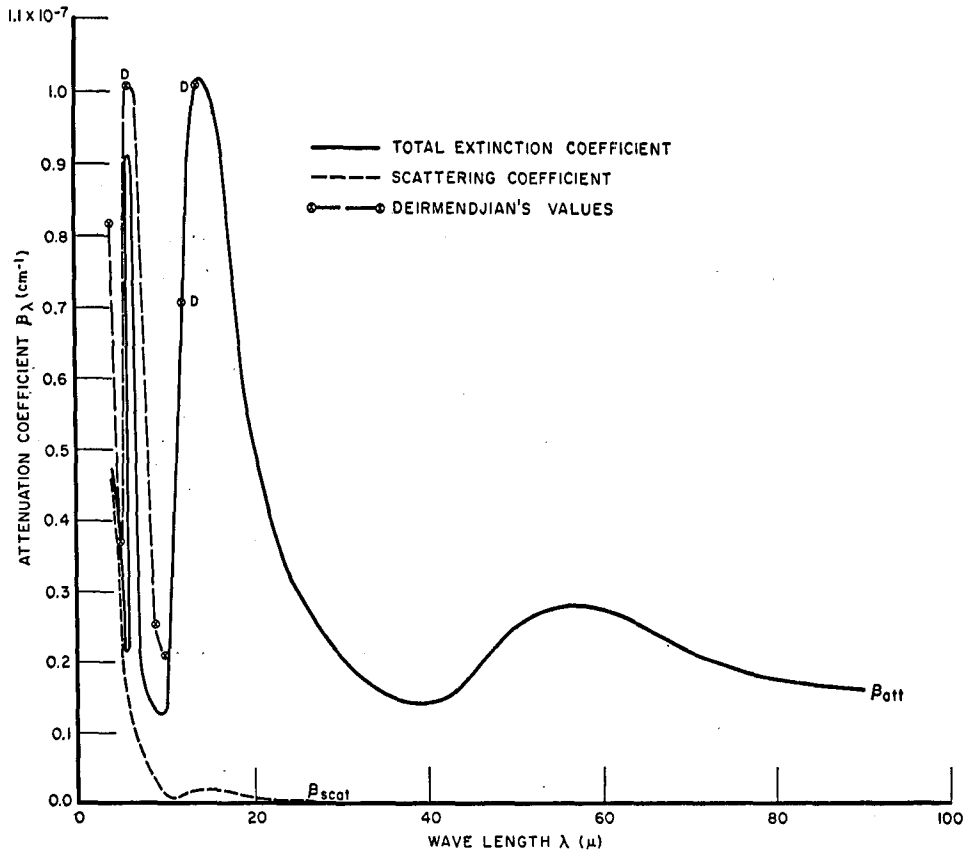

FIG. 1. Spectral distribution of the attenuation coefficients.

and (4)

$$n=2.251\times10^{-4}\ \ [\mathrm{cm}^{-3}\,\mu^{-1}]\ \ \text{for}\ \ r_1\leqq r\leqq r_0,$$

where $r_1=0.03$ micron, $r_0=0.10$ micron, and $r_2=2$ microns, as used by Deirmendjian. The monochromatic extinction efficiency factor Q_{ext}, is obtained from the truncated van de Hulst series as defined by

$$Q_{ext}\doteq \mathrm{Im}\left\{4\alpha\left[M+\frac{\alpha^2}{15}M^2\left(\frac{m^4+27m^2+38}{2m^2+3}\right)\right]\right\}+\frac{8}{3}\alpha^4\,\mathrm{Re}\left\{\left(\frac{m^2-1}{m^2+1}\right)\right\}. \quad (5)$$

Here Im and Re stand for the imaginary and real part of the argument. The complex index of refraction m was obtained from Stephens (1961). The quantity M is

$$M=\frac{m^2-1}{m^2+2}. \quad (6)$$

The attenuation coefficient for scattering is defined analogously, but Q_{ext} is replaced by Q_{scat} as defined by

$$Q_{scat}\doteq\frac{8}{3}\alpha^4|M|^2. \quad (7)$$

The truncated van de Hulst series are only valid for α less than 0.6. For size parameters greater than 0.5, efficiency factors were obtained from Stephen's Mie computations by means of a non-linear interpolation. All attenuation coefficients were obtained by means of an electronic computer.

The results are shown in Fig. 1. The total extinction coefficient varies only one order of magnitude while the water vapor absorption coefficient varies by at least five orders of magnitude. Therefore, the extinction coefficient for haze as compared to the absorption coefficient for water vapor may be considered as approximately grey at least beyond 25 microns. It is of interest to note that the haze absorption coefficient has a relative minimum at about 10 microns which is the region where the maximum emission of the earth's surface takes place. The scattering coefficient is shown also, and is identical with the total extinction coefficient at approximately 4 microns, which is equivalent to stating that the absorption coefficient is approximately zero. For increasing wavelengths the scattering coefficient vanishes so that the entire attenuation is due to absorption. For comparison, Deirmendjian's (1960) attenuation curve which only goes to 14 microns is shown also. Small deviations are probably due to slightly different values of the refractive index.

TABLE 1. Spectrally averaged attenuation coefficients $\bar{\beta}_{o,att}$, $\bar{\beta}_{o,abs}$, and $\bar{\beta}_{o,scat}$, 4.0–90.0 microns.

Temperature (°K)	Attenuation factors $\bar{\beta}_{o,att}$ (cm^{-1})	$\bar{\beta}_{o,abs}$ (cm^{-1})	$\bar{\beta}_{o,scat}$ (cm^{-1})
290	4.666×10^{-8}	4.425×10^{-8}	0.241×10^{-8}
260	5.156×10^{-8}	5.057×10^{-8}	0.099×10^{-8}
230	4.946×10^{-8}	4.820×10^{-8}	0.126×10^{-8}
200	4.788×10^{-8}	4.694×10^{-8}	0.094×10^{-8}

Since the emissivity for water vapor $\epsilon(w)$, which is treated as independent of wavelength, is used in the computation of the radiative flux divergence, it will be required to obtain a wavelength independent haze coefficient. For the total radiation the monochromatic attenuation coefficient β_0 is then replaced by a spectrally averaged attenuation coefficient $\bar{\beta}_0$ as defined by

$$\beta_0=\frac{\pi\int_0^\infty B_\lambda(T)\beta_0(\lambda)d\lambda}{\pi\int_0^\infty B_\lambda(T)d\lambda}, \quad \text{where} \quad \pi\int_0^\infty B_\lambda(T)d\lambda=\sigma T^4, \tag{8}$$

and B_λ is Planck's function. It was found that $\bar{\beta}_0$ is only slightly temperature dependent allowing an average value to be used. Typical values for $\bar{\beta}_0$ are shown in Table 1.

3. Computational methods

In order to determine the fluxes it is useful to refer to Fig. 2. The total water vapor path length from the top of the atmosphere to the ground is U, and the path length from the top of the atmosphere to the reference level is u. Analogously, D^* and D are defined as the haze mass. If w and μ define the absorbing masses from the top of the atmosphere to any elemental layer for water vapor and haze, respectively, the flux dF originating from an elemental layer above the reference level is then given by Zdunkowski *et al.* (1965) as

$$dF=\sigma T^4\left\{\left|\tau(L(D-\mu))d\epsilon(w)\right|+\left|\frac{K_a}{L}\tau(u-w)d\tau(L\mu)\right|\right\}. \tag{9}$$

Whenever the transmission τ is a function of μ, it takes into consideration the effect of haze absorption, as well as primary scattering. Due to the smallness of the scattering coefficient, it is permissible to neglect higher order scattering. Had the scattering effect been omitted altogether, only a small error would have resulted. The ratio of the absorption coefficient K_a to the total extinction L is 0.97, using an average temperature, which proves this point of view. The net flux at a reference level h in the atmosphere is given by the upward flux minus the downward flux according to (10),

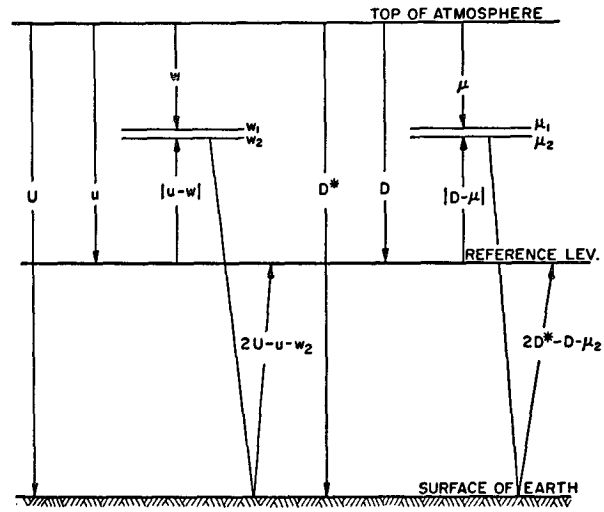

FIG. 2. Integration of radiative fluxes.

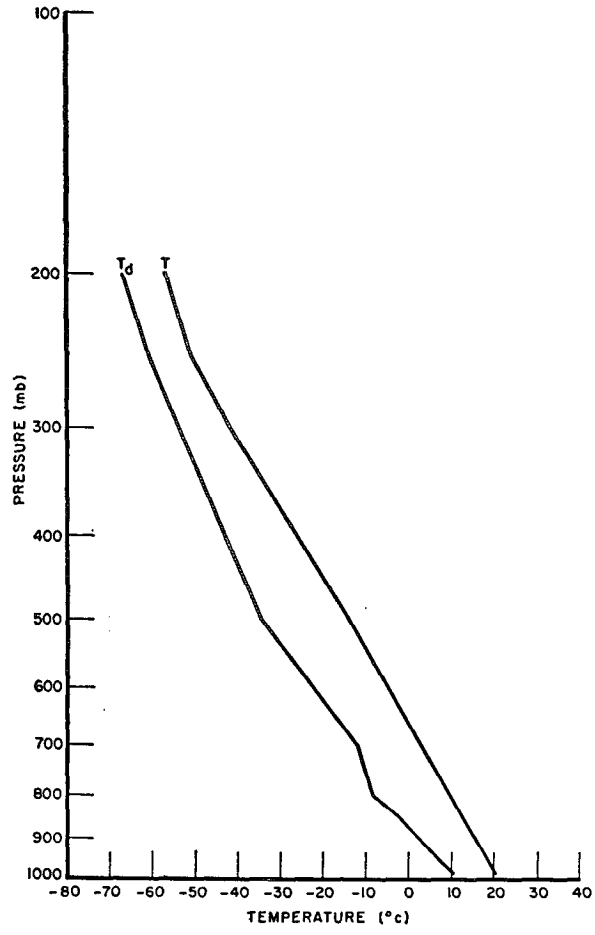

FIG. 3. Temperature and dew-point distribution of the free air.

$$F_N(h)=\epsilon_s\sigma T_s^4\tau[L(D^*-D)]_\tau(U-u)$$
$$+r\sum_{i=1}^{j}\Delta F_{\text{refl}}(w,\mu,T)+\sum_{i=1}^{h}\Delta F(w,\mu,T)$$
$$-\sum_{h}^{j}\Delta F(w,\mu,T). \quad (10)$$

The upward flux consists of three components. The first component is the emission of the surface which is attenuated by the haze and water vapor between the surface and the reference level. If the surface is assumed to be grey instead of black, the surface emissivity is denoted by ϵ_s, i.e., $1-r$. The second component, represented by the second term on the right hand side of (10), is the radiation reflected by the surface as illustrated by Fig. 2 and given by:

$$\Delta F_{\text{refl}}(w,\mu,T)$$
$$=\sigma T_s^4\left\{\tau_\mu\left[\left(2D^*-D-\frac{\mu_1+\mu_2}{2}\right)\right]\right.$$
$$\times[\epsilon_w(2U-u-w_1)-\epsilon_w(2U-u-w_2)]$$
$$+\frac{K_a}{L}\tau_w\left(2U-u-\frac{w_1+w_2}{2}\right)$$
$$\left.\times[\tau_\mu(2D^*-D-\mu_2)-\tau_\mu(2D^*-D-\mu_1)]\right\}. \quad (11)$$

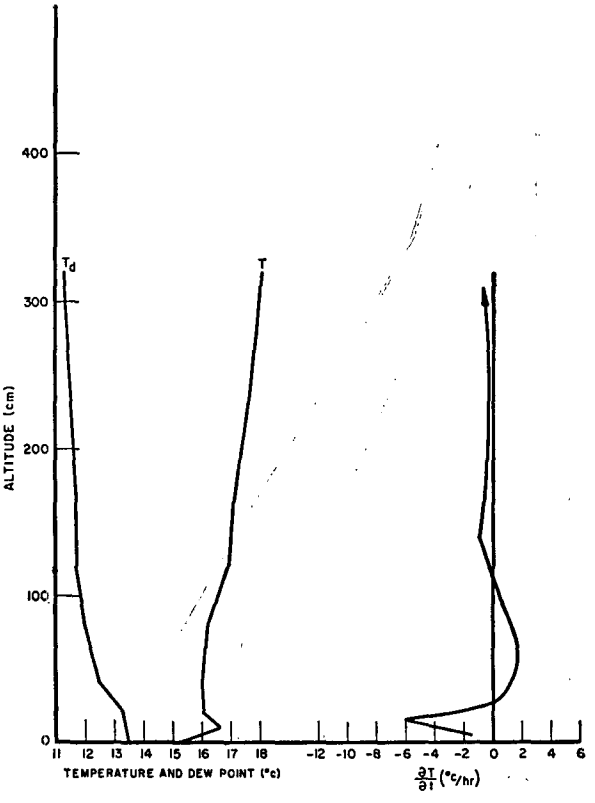

FIG. 4. Low-level temperature and dew-point distribution and corresponding water vapor radiative cooling rate.

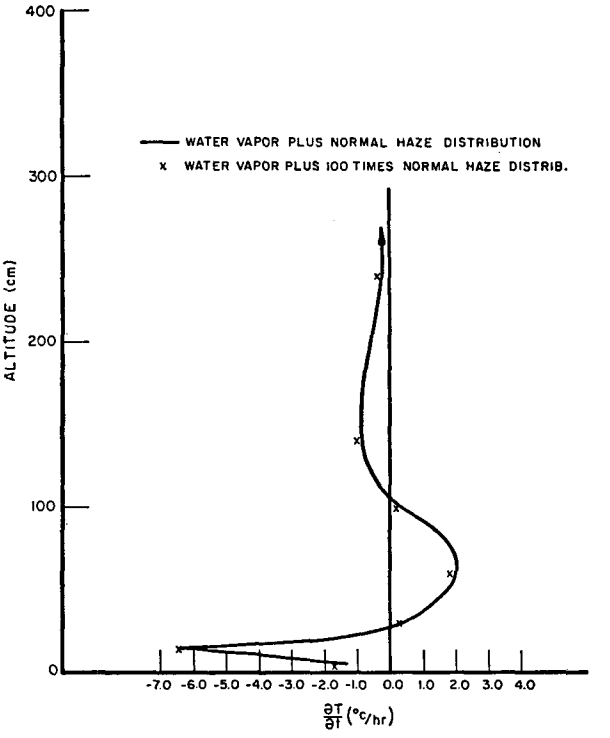

FIG. 5. Low-level radiative cooling rates for water vapor plus haze.

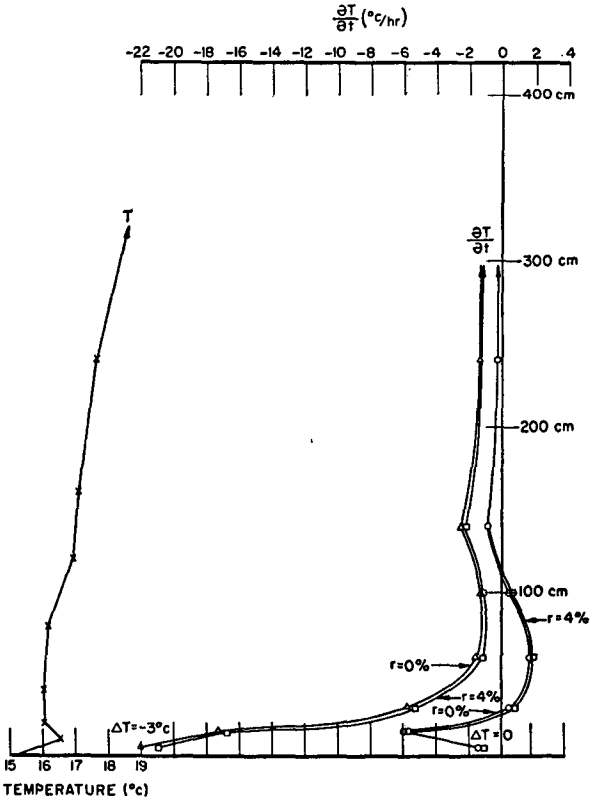

FIG. 6. Low-level radiative cooling rates including reflectivity and surface temperature discontinuity.

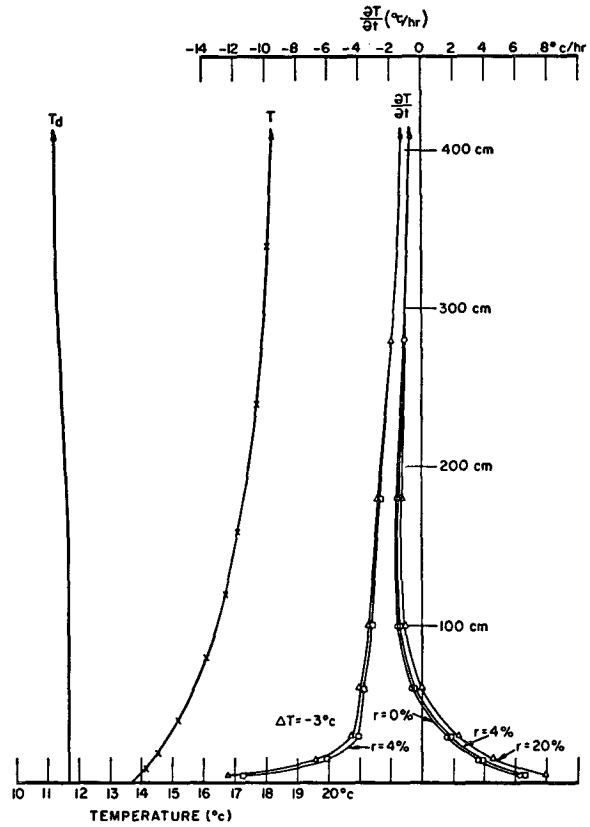

FIG. 7. Low-level nighttime temperature and dew-point distribution and associated radiative cooling rates for a water vapor atmosphere with surface temperature discontinuity and surface reflection.

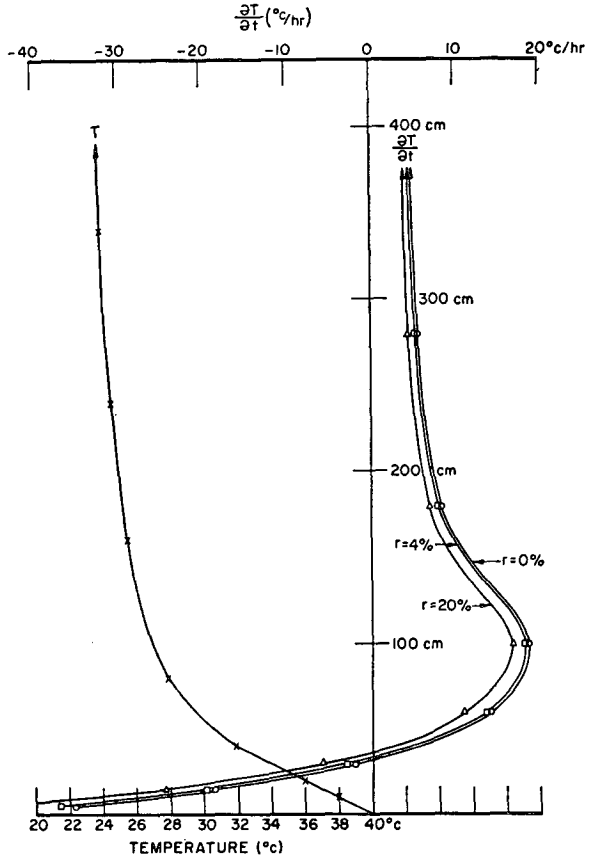

FIG. 8. Low-level daytime temperature distribution and associated cooling rates for $r=0$, 0.04, and 0.20.

The summation from $i=1$ to j includes all downward flux contributions from the entire atmosphere, and T_e represents the effective temperature of a given layer. The third component stands for the upward flux emitted by the water vapor-haze atmosphere between the surface of the earth and the reference level which is indicated by summation $i=1$ to h. The downward flux at the reference level is then found by summing the fluxes from h to j.

4. Results

The effect of haze is investigated using observed as well as hypothetical soundings. The temperature and moisture distribution observed in the free air was assumed to be the same in all cases and is shown in Fig. 3. Reasonable variations of the adopted free air observations have only small effects upon surface boundary computations. A typically observed case, not necessarily representative, is shown in Fig. 4 for water vapor absorption only. Introducing a normal continental haze distribution with 1.8 km for H, the resultant cooling curve, in Fig. 5, cannot be distinguished from that for water vapor alone (Fig. 4). Introducing one hundred times as much haze without changing the particle size distribution results in a new cooling curve as indicated by the crosses. As can be seen, no significant changes are found. It should be noted that neither a surface temperature discontinuity nor the reflection of the surface is taken into consideration.

Next, it will be shown that a temperature discontinuity and a non-zero infrared albedo (particularly the former) are far more effective in changing the cooling rate at very low levels than any reasonable haze distribution. This does not include any small layer of highly concentrated surface haze or a radiation fog.

Inspection of Fig. 6 (no haze included) reveals that the assumed temperature discontinuity of −3C has a profound influence upon temperature changes. A surface reflectivity of 4 per cent is of less importance.

In order to eliminate the effect of temperature irregularities, computations were made from a smoothed low level temperature distribution which closely resembles observed temperature profiles during the night. The results are shown in Fig. 7. Going from left to right, one recognizes the strong effect of the surface temperature discontinuity which changes radiative heating to radiative cooling. The effect of reflection ($r=0.04$) is small, but it indicates the tendency of greater heating than would occur otherwise. This is due

to the strong low level inversion. A surface reflectivity of 20 per cent (Yamamoto and Kondō, 1959) which is undoubtedly too high, changes the flux divergence by roughly 20 per cent. It should be noted that the haze effect is not included.

In order to further investigate the effect of reflectivity upon infrared flux divergence, a sounding representing the temperature distribution at the time of maximum solar heating was used and results are shown in Fig. 8. Reflection results in additional cooling of roughly 20 per cent for $r=0.20$ while for the inversion case, reflection resulted in heating.

The exponential haze distribution of Fig. 5 is used for the inversion case with results shown in Fig. 9. Comparison with Fig. 7 (note different height scales) reveals that one hundred times the normal haze distribution results in an additional one-half degree cooling per hour. During the nighttime a surface reflectivity of 4 per cent has about the same effect on radiation temperature changes but of opposite sign. Since these cooling rate profiles above 40 cm rapidly approach the corresponding profiles of Fig. 7, the computations were discontinued at that height.

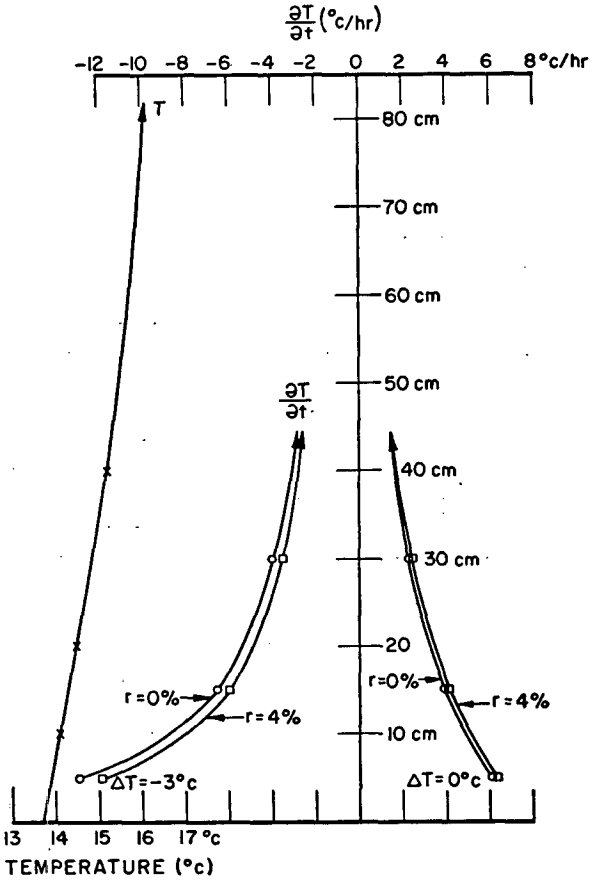

FIG. 9. Low-level nighttime radiative cooling rates with water vapor plus 100 times normal exponential haze distribution including surface temperature discontinuity and surface reflection.

What then is the haze effect upon the cooling rate in the free atmosphere? Fig. 10 explains this effect. One hundred times the normal haze distribution approximately doubles the cooling rate due to water vapor alone in the lower part of the troposphere, while the normal haze distribution has no appreciable effect. In the upper troposphere the cooling profiles approach each other due to the exponential decrease of the haze. Twenty-five times the normal distribution is almost as effective in producing additional radiative cooling as one hundred times the normal haze distribution. This is due to the fact that the cooling of the atmosphere cannot be increased indefinitely by increasing the turbidity of the air. A very heavy amount of haze will approximate a cloud where the cooling becomes almost zero due to the blocking effect of the outgoing radiation.

Another question that must be asked is: how reasonable is a continuous haze distribution of one hundred times the normal concentration? To clarify this, the downward fluxes are computed and illustrated in Fig. 11. The downward flux at the surface due to water vapor alone is roughly 0.33 cal cm^{-2} min^{-1}, while the downward flux for one hundred times the normal haze distribution is approximately 0.51 cal cm^{-2} min^{-1}, i.e., an increase of 55 per cent.

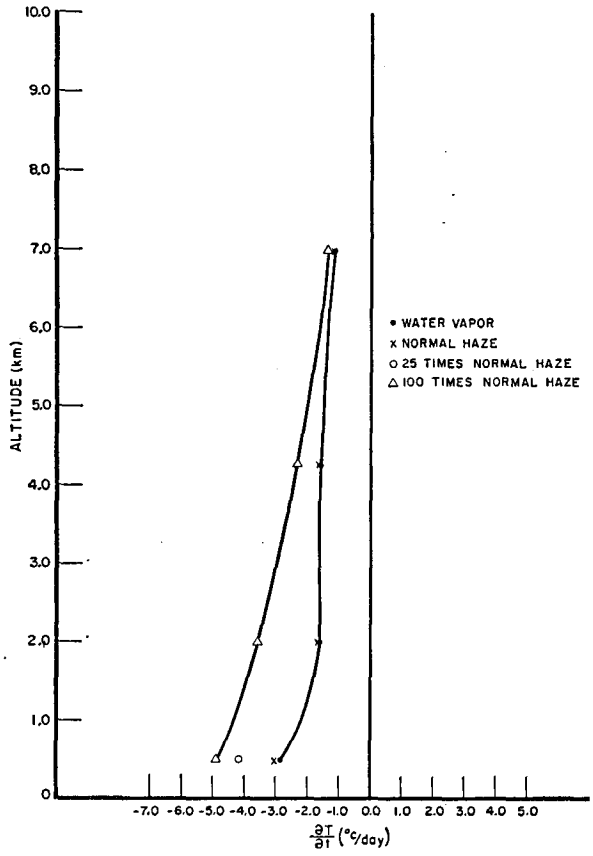

FIG. 10. High-level radiative cooling rates for water vapor and water vapor plus haze atmospheres.

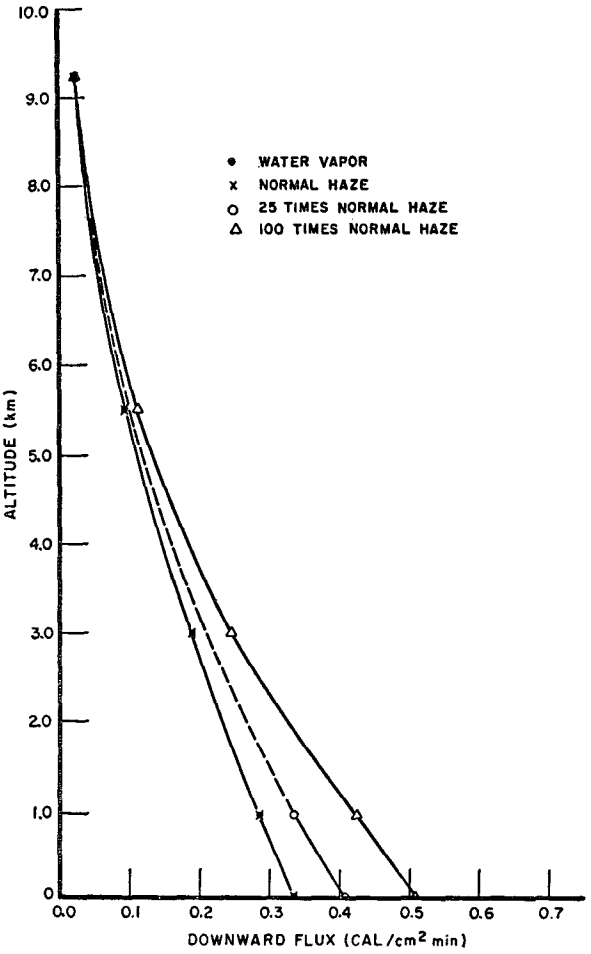

FIG. 11. Downward flux for water vapor and water vapor plus haze atmospheres.

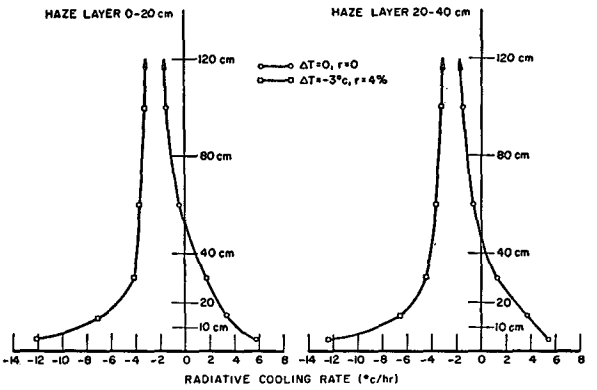

FIG. 12. Low-level radiative cooling rates for water vapor plus layered haze including surface temperature discontinuity and surface reflection.

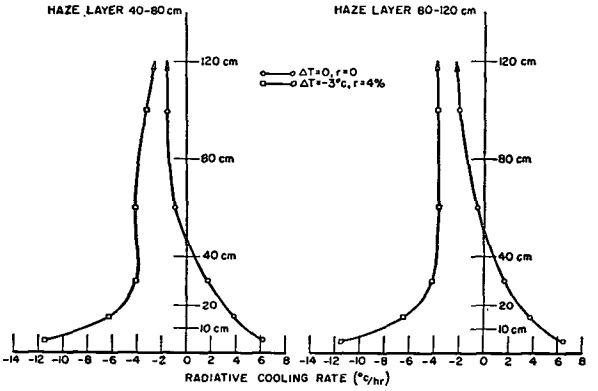

FIG. 13. Low-level radiative cooling rates for water vapor plus layered haze including surface temperature discontinuity and surface reflection.

The water vapor emissivity used for these calculations was taken from Kuhn (1963) who took great precaution to avoid the influence of haze upon his emissivity curve. According to Brooks (1950), a fairly hazy atmosphere, as might be observed under anticyclonic conditions, might increase the downward flux by 8 to 10 per cent. Increasing the normal haze distribution by twenty-five times yields an increase of 20 per cent of the downward flux, while ten to fifteen times as much haze results in an 8 to 10 per cent increase of the downward flux.

The effects of layer haze shall be discussed briefly assuming that all haze is concentrated in small layers near the surface with no haze above or below. For these calculations the sounding in Fig. 7 was used. In order to estimate the maximum effects, one hundred times the normal haze distribution was used, which results in a visual range of slightly less than 0.5 km. Calculations were made by positioning the haze layers as indicated in the appropriate figures.

A study of Figs. 12 and 13 indicates that layer haze of this concentration will not essentially influence the cooling of the air. The effect of a −3C surface temperature discontinuity is of a higher order of magnitude. Apparently these results contradict those reported by Möller (1964). He finds, for a haze layer 30 cm thick overlying the surface, using the U. S. Standard Atmosphere, and 75 per cent relative humidity, a cooling rate ten times as large as the haze free air directly above. Using his data it was found that a pure haze atmosphere with no water vapor present gives a cooling rate approximately seven times larger than the water vapor-haze atmosphere, thus, the presence of water vapor reduces the cooling rate due to haze substantially. His absorption coefficient for haze was ten times as large as the one used here and is indicative of cooling rates in a fog layer already formed. Hence, there is no contradiction between Möller's and these results. The transition from a haze layer to a fog layer apparently takes place when the extinction coefficient used here is increased by a power of ten.

5. Conclusions

The computations indicate that Deirmendjian's continental haze distribution could be ten times as concentrated without increasing the downward flux sig-

nificantly beyond the observed values. The increased energy arriving at the surface may be significant for the heat budget of the soil, but it does not significantly increase the radiative cooling rate near the surface. However, Zdunkowski (1963) pointed out that a haze layer in the higher parts of the troposphere, with low water vapor concentration, will produce abnormal radiative heating and cooling. The assumption that the haze consists of water droplets is reasonable especially when high relative humidities are involved. This conclusion can be substantiated from Volz's (1957) measurements covering the infrared spectrum to approximately 15 microns. The effect of dry haze, after Volz, is even less critical upon the infrared cooling rates. It may be inferred that concentrated haze layers near the surface, imbedded in a continuous haze distribution, will also be of little importance.

Funk (1960), comparing measured and theoretically obtained flux divergence, finds serious disagreement. He attributes this to the presence of haze invisible to the naked eye. If haze particles are really well represented by the complex index of refraction of water, then Funk's conclusion seems doubtful, providing the water vapor emissivities for very small path lengths are approximately correct. Based on energy budget considerations Kraus (1963) expressed serious doubts about Funk's conclusion, and is of the opinion that such effective haze would be visible. Radiative temperature changes for water vapor atmospheres based on extrapolations from free air and laboratory measurements, as well as radiation charts, give similar results. It is highly improbable that the presence of carbon dioxide will be responsible for the observed discrepancy, although actual computations of carbon dioxide influence near the surface are not yet available.

Using a somewhat different haze particle distribution function, with a number of larger particles, will not give greater absorptivity of the haze than one hundred times the value found, as may be judged from Deirmendjian's (1960) extinction curves. The effect of such aerosols, which cannot be reasonably approximated by water droplets, is not known and may partly account for Funk's discrepancy.

After fog formation the droplet effect will be dominating and cooling rates as large as observed by Funk may be calculated. It may also be concluded that it is more important to know the exact surface temperature than an exact description of the distribution function of haze particles which behave like water droplets.

Acknowledgments. The authors express sincere gratitude to Drs. Helmut Weickmann and Robert Fenn for for their interest in the study, as well as for their helpful suggestions, which resulted in obtaining new information contained in the literature which may not have been detected otherwise. We are also indebted to Prof. F. Möller for his discussion on the subject and to the referees for their critical review.

REFERENCES

Brooks, D. L., 1950: A tabular method for the computation of temperature change by infrared radiation in the free atmosphere. *J. Meteor.*, **7**, 313–321.

Deirmendjian, D., 1959: The role of water particles in the atmospheric transmission of infra-red radiation. *Quart. J. R. Meteor. Soc.*, **85**, 404–411.

——, 1960: Atmospheric extinction of infra-red radiation. *Quart. J. R. Meteor. Soc.*, **86**, 371–381.

Fleagle, R. G., 1953: A theory of fog formation. *J. Marine Res.*, **12**, 43–50.

Funk, J. P., 1960: Measured radiative flux divergence near the ground at night. *Quart. J. R. Meteor. Soc.*, **86**, 382–389.

Kraus, H., 1963: Der Tagesgang des Energiehaushaltes der bodennahen Luftschicht. *Arch. Meteor. Geophys. Bioklimat., Series B*, **12**, 491–515.

Kuhn, P. M., 1963: Radiometersonde observations of infrared flux emission of water vapor. *J. Appl. Meteor.*, **2**, 368–378.

Möller, F., 1955: Strahlungsvorgänge in Bodennähe. *Z. Meteor.*, **9**, 47–55.

——, 1964: Einige Überlegungen zur Frage des abgehobenen Temperaturminimums bei Nacht. *Meteor. Rund.*, **17**, 86–89.

Stephens, J. J., 1961: Spectrally averaged total attenuation, scattering, and absorption cross-sections for infrared radiation. *J. Meteor.*, **18**, 822–828.

Volz, F., 1957: Die spektralen Eigenschaften der Dunstsubstanz: UV-Absorption von Niederschlagswasser und der Dunsteinfluss auf die langwellige atmosphärische Strahlung. *Ann. Meteor.*, **8**, 34–40.

Yamamoto, G., and J. Kondō, 1959: Effect of surface reflectivity for long wave radiation on temperature profiles near the bare soil surface. *Science Reports of the Tohoku University*, Series 5, Geophysics, **11**, No. 1, 9 pp.

Zdunkowski, W. F., 1963: Untersuchungen über die langwellige Strahlung der Atmosphäre. *Ger. Beit. Geophys.*, **72**, 103–106.

——, D. Henderson, and J. V. Hales, 1965: The influence of haze on infrared radiation measurements detected by space vehicles. *Tellus*, **17**, 147–165.

——, and F. G. Johnson, 1965: Infrared flux divergence calculations with newly constructed radiation tables. *J. Appl. Meteor.*, **4**, 371–377.